



## Curve-based image editing for product styling

Bo Wang <sup>a</sup>, Bao-Jun Li <sup>a</sup>, Franca Giannini <sup>b</sup>, Marina Monti <sup>b</sup>, Ping Hu <sup>a</sup> and Ji-Cai Liang <sup>a</sup>

<sup>a</sup>DaLian University of Technology, China; <sup>b</sup>IMATI - CNR, IT

### ABSTRACT

This paper presents an approach for curve driven image warping to reshape the content of an image. The warping method is realized by inverse irregular quad mesh mapping. Considering that stylists adopt a curve based approach for their product shape definition, the devised curve driven image warping can provide a good mean for rapidly changing the product shape, thus easing the evaluation of shape alternatives. Moreover, here we show that the semantically editing of automotive images can be easily implemented combining this method with the automatic identification of the semantically important character lines.

### KEYWORDS

Curve driven image modification; image warping; inverse mapping; product styling

## 1. Introduction

In image processing, image warping typically is applied to remove distortions from an image, but it is also used for artistic purposes and special effects in interactive paint programs. Additionally it could offer a valid support for design activities in fast outlining potential design solutions if suitable editing capabilities are provided. In fact, in early design activities, stylists are used to take inspiration from already existing products or elements present in nature. Therefore it would be useful if the large amount of digital images available on the web or easily obtainable by personal camera, could be directly used for the specification and visualization of new shapes. Image warping is the act of distorting a source image into a destination image according to a mapping between the source space  $(u, v)$  and the destination space  $(x, y)$ . The forward mapping is usually specified by the functions  $x(u, v)$  and  $y(u, v)$ , but potential gap problems exist. Better results can be obtained applying the inverse mapping to find the corresponding location in the original image for every pixel in the destination image.

Image morphing [1] [16] is an implementation of image warping. Several methods and technologies are applied in image morphing: triangulation based morphing, mesh warping, field morphing, moving least square and as-rigid-as-possible usually applying some energy minimization approach.

Among the various works present in literature aimed at modifying an image while considering constraints dependent on the image content, [10] retargets an image

to preserve shapes of both visually salient objects and structure lines while minimizing visual distortions. [6] deforms and combines image regions by optimizing a shape distortion energy, while [12] minimizes the energy function in the gradient vector flow field. [9] minimizes the deformation energy defined in Euclidean space as rigid as possible. [15] presents a “scale-and-stretch” warping method that allows resizing images into arbitrary aspect ratios while preserving visually prominent features. Even if proving good results these works cannot be used for supporting designers, since they address the resize of the image, while for designers it is very important not only to localize but also to drive the image changes on specific areas, possibly using as modification handles meaningful elements such as the characteristic lines of the object under modification.

A more localized user driven image warping method is presented in [17]. This work shows an easy-to-use image retouching technique for realistic reshaping of human bodies in a single image, driven by a 3D whole-body morphable model. However, it is only applicable to objects whose local modification can be directly driven by numerical parameters, such as the human body, and it is not immediately extendable to arbitrary objects.

For styling products, such as consumer appliances or cars, their parameterization is not easy and it involves high-level parameters, such as the characteristics lines [7]. In this perspective, [14] introduces a method to reshape car body images driven by a morphable model of parametric curves. Unfortunately, this method is a little

complex since it requires the decomposition of the car body into patches with four edges to use Ferguson function and potential texture gap problems are inevitable.

To improve the curve-based image warping in the product design context, this paper shows a method to get image modification driven by curves, while eliminating the constraints related to the number of the edges limiting the deformed areas. With a regular sparse matrix, the optimized warped result can be computed directly by solving the matrix function.

The contributions of this paper with respect to previous works are:

- No limitations on the warping region: it is not restricted to be quadrilateral. Reshaping one curve inside or outside an arbitrary region can be realized. Thus, the number of the constraint curves is not limited. In addition, the region is also not restricted to be closed;
- Reduction of the complexity by avoiding the decomposition of the image to Ferguson patches to maintain the reshaping effects of the curved edges;
- Solving a sparse matrix instead of minimizing an energy function for image deformation.

Our goal is to provide an easy image warping scheme driven by curve modification. To this aim, the method described in this paper uses irregular meshing for the destination image according to the constraint curves firstly; secondly, it applies the inverse mapping obtained by solving a sparse matrix. The method has been tested for the modification of car images through the editing of the related automatically detected main character lines, as well as on images of other products and subjects.

Section 2 introduces the adopted automatic method to extract the parametric curve model for a car body. Section 3 presents the main algorithms to realize the curve driven warping method. Section 4 illustrates some results obtained by the application of the described method and conclusions are given in Section 5.

## 2. Automatic extraction of parametric curve model

To effectively support designers in exploiting images for the evaluation of product shape alternatives, it is important to provide them an easy access to the most prominent features usable as handles/parameters both to modify the image and to create the digital model of the chosen product version. In this section, we introduce the role of the Computer-Aided Design representation for product shape definition and describe the devised method for the automatic detection from images of the most important

characteristic curves adopted by designers to specify the wished car shape.

The creation of the product model with Computer-Aided Design (CAD) systems is one part of the whole digital product development activity within the product lifecycle management process. The creation of the digital model of the product shape is performed in different ways depending on the user skill (stylists vs engineers) and on the type of software adopted [3]. Usually, 2D drawings are used by designers and stylists to specify their ideas, while 3D parametric modeling is used for detailed design, analysis and production. 2D vector drawings are also used as the baseline to create 3D models for many industrial design products. Among them, automotive designers make a large use of drawing and sketches, either hand-made or digital, as the first step to project a new car. With the purpose to support all users to edit car images easily, we recover from lateral images the parametric curves corresponding to the main character lines representing the most important curves created by designers to provide the car aesthetic character [4]. A template model (Fig. 1) is used in which characteristic curves are decomposed in shorter elements to better adapt to the car shape variations. For the definition of the template model we investigated various types of cars, finally we chose a template model corresponding to a SUV car since from the performed tests it demonstrated to best suit to the various car categories. These character curves are referred as key curves, whose extrema are denoted as key points.

### 2.1. Curve model extraction from images

The proposed approach for the automatic recovery and annotation of editable characteristic curves from images consists of a series of processes aimed firstly at cleaning and making compatible the edge curves detected in the image with the template and secondly at constructing the important curves corresponding to those present in the template. To avoid size problems, images are normalized to a standard size (width = 1500). The applied edge detection algorithm identifies the important edge points using a combination of the SFE [5] and Canny [2] methods, and clusters them into chains of consecutive points (see Fig. 2).

Chains are split into elementary chains to obtain pieces with low curvature variation that can be well approximated by quadric curves with the fitting error of each piece less than a given threshold (here set to 3). Quadric curves rather than cubic curves are used because simpler and sufficient to approximate the few smooth subparts with coherent curvature in which the characteristic curves of a car can be decomposed. Smallest chains are

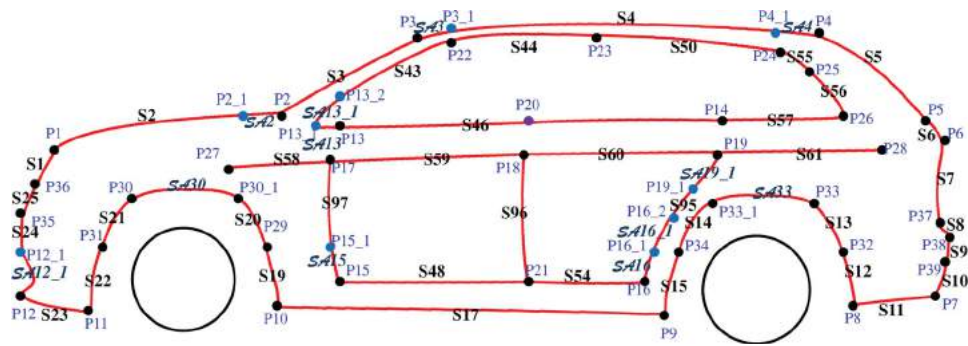


**Figure 1.** The adopted 2D parametric template representing the main character lines of a car.

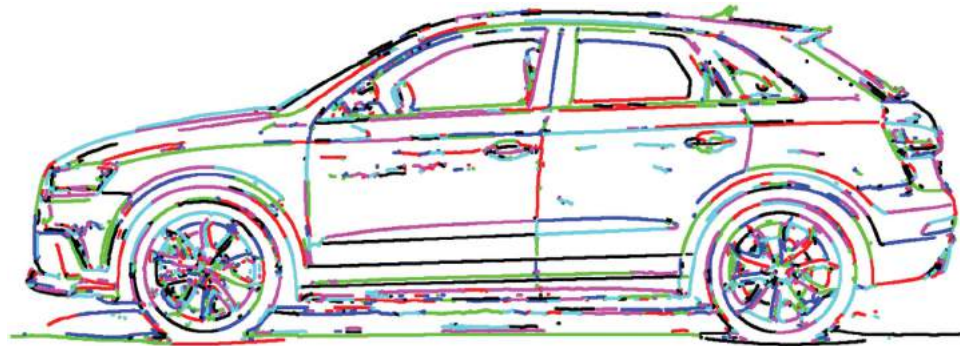


**Figure 2.** Point chains, different colors represent different chains.

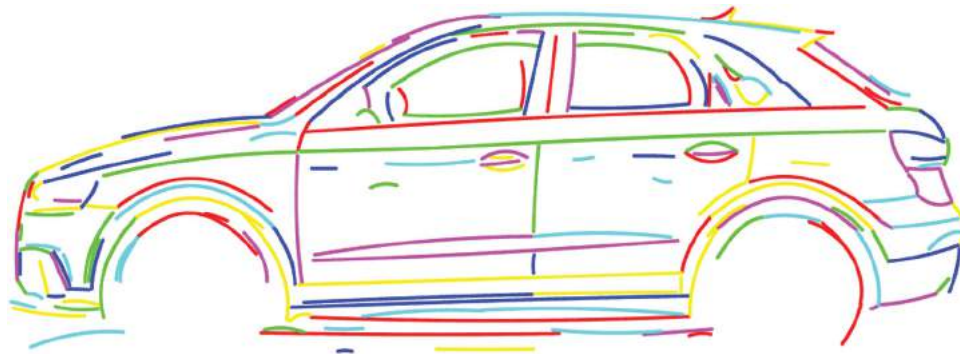


**Figure 3.** Quadric curves from the feature points. Different colors represent different quadric curves.

removed, since they normally correspond to less important details, as lights or shadows. The remaining chains are then used to identify wheel curves and centers, which are the exploited for the registration of the template model to the image. Wheels are the parts with a specific shape (i.e. circle) always present in car body; they usually are easily extracted because of the big difference in color of the rim with respect to the tires. The Hough transform algorithm [8] is used to detect them.

Chains internal to the detected wheel curves are removed. The remaining elementary chains are then combined together to longer quadric curves (Fig. 3) considering a larger fitting error threshold ( $= 5$ ), thus obtaining curves more similar to the ones in the image.

The wheel curves and centers are used as constraints for the template registration based on the PR-GLS algorithm [11].

Finally, the curves corresponding to the ones of the template are created, exploiting the registered template key points, imposing the widest coverage of the image edge points, and other conditions peculiar to each specific character curve of the car. A candidate region for every key point in the image is computed from the position of the registered model key points. Candidate curves between two key points can be selected from the computed quadric curves that intersect the region included in the parallelogram between the corresponding registered points (Fig. 4).

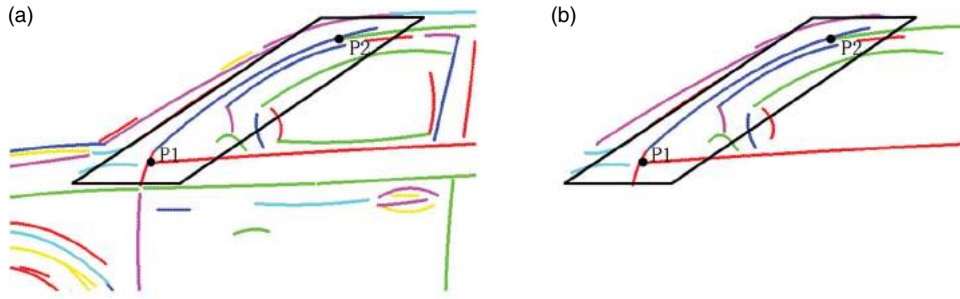


**Figure 4.** Candidate quadric curves between two registered key points. (a) parallelogram region R created from two key points and all the quadric curves in the surrounding image area; (b) candidate quadric curves intersecting the region R.

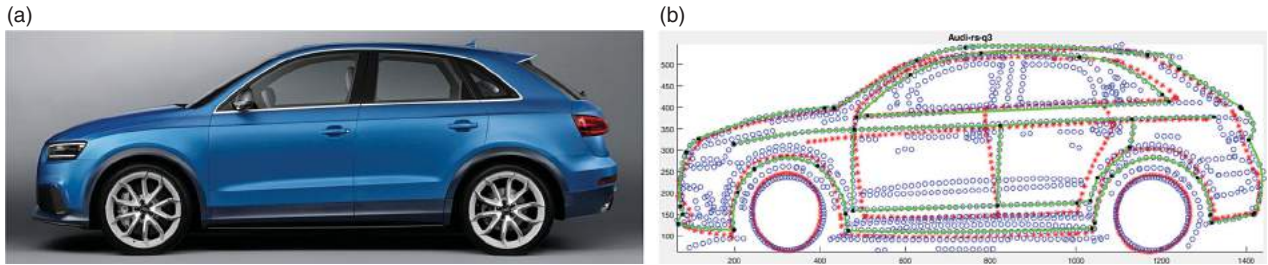


**Figure 5.** An example of the obtained model matching. In (b), blue points are the image edge points; red points are points of the warped template model; green lines are the obtained curves; black points are the obtained key points.

The final character curves are those having the largest coverage of the image feature points and satisfying their specific shape and position constraints.

Figure 5 shows the fully automatic result we obtained for an Audi RS Q3 car downloaded from Google images.

Since Bézier curves are more used in CAD design providing more efficient modification capabilities and more freedom in the achievable shapes than quadric curves, finally the quadric curves are refitted to a cubic Bézier curve.

### 3. Curve driven image warping

In the following, *ImgSource* refers to the source image and *ImgWarp* indicates the destination image. Conceptually the warping of *ImgSource* to *ImgWarp* is obtained by considering in *ImgSource* the original characteristic curves used as modification handles and in *ImgWarp* the modified curves; that is the warping results from reshaping the curves in *ImgSource* to the curves in *ImgWarp* and modifying accordingly the related pixels and those in the surrounding image area. The adopted notations to describe the method are given in Tab. 1.

#### 3.1. Curve correspondence

In order to obtain a uniform warping effect, we arrange the correspondence of the curve points according to

**Table 1.** Notations for the curves in the two images.

	Cubic Bezier curves	endpoints
<i>ImgSource</i>	$\{SC^k\}_{k=1}^{N1}$	$\{BeginP\_SC^k\}_{k=1}^{N1}, \{EndP\_SC^k\}_{k=1}^{N1}$
<i>ImgWarp</i>	$\{WC^k\}_{k=1}^{N1}$	$\{BeginP\_WC^k\}_{k=1}^{N1}, \{EndP\_WC^k\}_{k=1}^{N1}$

their distance with respect to their endpoints. Given a curve  $WC^k$  we consider its points  $\{Q_j^k\}_{j=1}^{NQ_k}$ , such that the arc distance of two close points is less than 2. We apply the same method to  $SC^k$  to obtain the set of points  $\{P_i^k\}_{i=1}^{NP_k}$ . For each  $Q_j^k$ , the corresponding  $P_{i(j)}^k$  is selected according:

$$i(j) = \min_i \left| \frac{|P_i^k - BeginP\_SC^k|}{|EndP\_SC^k - BeginP\_SC^k|} - \frac{|Q_j^k - BeginP\_WC^k|}{|EndP\_WC^k - BeginP\_WC^k|} \right| \quad (1)$$

Then the correspondence is built as

$$\left\{ P_{i(j)}^k \right\}_{j=1}^{NQ_k} \rightarrow \left\{ Q_j^k \right\}_{j=1}^{NQ_k}$$

#### 3.2. Irregular rectangular meshing

Inverse warping is adopted to avoid potential gap problems. Supposing the mesh step is  $r$  ( $r = 4$  is selected in this paper). The constraint points we use are the curve points that are also grid points. To avoid losing too many



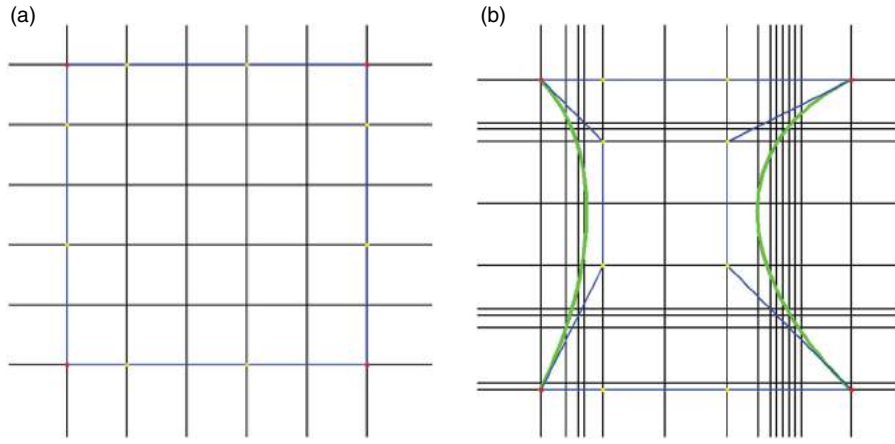


**Figure 6.** Constraint meshing grid. Blue lines are control lines of cubic Bezier curves. (a) is the meshing result with four straight curves; (b) is the meshing result with two straight curves and two bending curves.

$$Q(x_i, y_j) = \frac{(x_{i+1} - x_i)Q(x_{i-1}, y_j) + (x_i - x_{i-1})Q(x_{i+1}, y_j)}{x_{i+1} - x_{i-1}}$$

$$Q(x_i, y_j) = \frac{(y_{i+1} - y_i)Q(x_i, y_{j-1}) + (y_i - y_{i-1})Q(x_i, y_{j+1})}{y_{i+1} - y_{i-1}}$$

**Figure 7.** Relations between the points of the irregular mesh grid.

curve points, the mesh is refined near the curve points. When there are many curve points (10 is selected as the limit number in this paper) sharing the same  $x$  (or  $y$ ) value, then we add columns (rows) to the grid near that value, i.e. the grid is made denser along the  $x$  (or  $y$ ) axis near that value.

Fig. 6 shows examples of the meshing grid with different curve shapes.

### 3.3. Warping function

The constraint point set,  $WarpP$ , obtained from the warped curves as described in section 3.2, is then completed by adding the image boundary points as constraints to avoid distortions. The corresponding points set  $SampleP$  in  $ImgSource$  can be easily computed according to equation (1).

The inverse warping function is defined by:

$$F : ImgWarp \rightarrow ImgSource, \text{ s.t. } F(WarpP) = SampleP$$

The relationship matrix of the grid points is computed firstly. Suppose the mesh is:  $(x_1, x_2, x_3, \dots, x_M) * (y_1, y_2, y_3, \dots, y_N)$ .

Easily, with the relation of the irregular mesh grid points from Fig. 7, the relations in the source image can

be written as:

$$F(Q(x_i, y_j)) = \frac{(x_{i+1} - x_i)F(Q(x_{i-1}, y_j)) + (x_i - x_{i-1})F(Q(x_{i+1}, y_j))}{x_{i+1} - x_{i-1}} \quad (2)$$

$$F(Q(x_i, y_j)) = \frac{(y_{i+1} - y_i)F(Q(x_i, y_{j-1})) + (y_i - y_{i-1})F(Q(x_i, y_{j+1}))}{y_{i+1} - y_{i-1}} \quad (3)$$

With equations (2) and (3), the affine function can be rewritten as:

$$\begin{aligned} & \left( \frac{x_{i+1} - x_i}{x_{i+1} - x_{i-1}} \middle/ 2 \right) F(Q(x_{i-1}, y_j)) \\ & + \left( \frac{x_i - x_{i-1}}{x_{i+1} - x_{i-1}} \middle/ 2 \right) F(Q(x_{i+1}, y_j)) \\ & + \left( \frac{y_{i+1} - y_i}{y_{i+1} - y_{i-1}} \middle/ 2 \right) F(Q(x_i, y_{j-1})) \\ & + \left( \frac{y_i - y_{i-1}}{y_{i+1} - y_{i-1}} \middle/ 2 \right) F(Q(x_i, y_{j+1})) \\ & - F(Q(x_i, y_j)) = 0 \end{aligned}$$

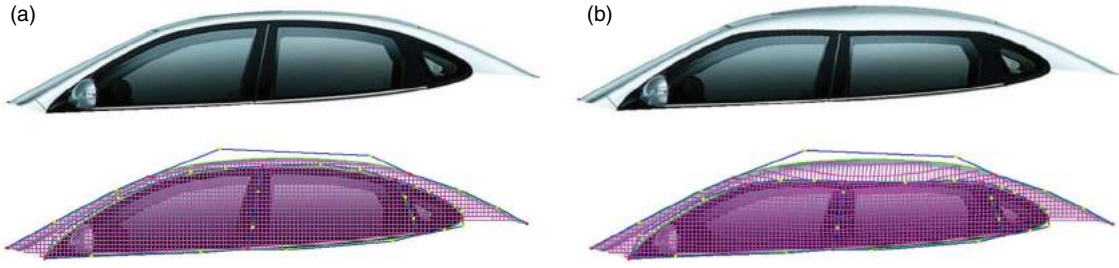


**Figure 8.** Example of warping result (b) obtained from (a).

These relations can be written as a sparse matrix:

$$T \begin{bmatrix} F(Q(x_1, y_1)) \\ F(Q(x_2, y_1)) \\ \vdots \\ F(Q(x_M, y_N)) \end{bmatrix} = B$$

Initialize  $T(M * N, M * N)$  as a unit matrix,  $B(1, M * N)$  as a zero vector. For point  $(x_i, y_j)$ ,  $k = y_j * M + x_i$ , if it is not a constraint point, then:

$$T(k, k - M) = -\frac{y_{i+1} - y_i}{y_{i+1} - y_{i-1}} \Big/ 2,$$

$$T(k, k - 1) = -\frac{x_{i+1} - x_i}{x_{i+1} - x_{i-1}} \Big/ 2,$$

$$T(k, k + 1) = -\frac{x_i - x_{i-1}}{x_{i+1} - x_{i-1}} \Big/ 2,$$

$$T(k, k + M) = -\frac{y_i - y_{i-1}}{y_{i+1} - y_{i-1}} \Big/ 2,$$

else

$$B(1, k) = F(Q(x_i, y_j))$$

It can be easily obtained from the constraint  $F(\text{WarpP}) = \text{SampleP}$ . Finally,  $T$  is a sparse matrix with the non-zero elements only at  $T(k, k - M + 1)$  ( $k \geq M$ ),  $T(k - M + 1, k)$  ( $k \geq M$ ),  $T(k, k + 1)$ ,  $T(k + 1, k)$ .

### 3.4. Matrix solution

Usually, the sparse matrix  $T$  is large with size  $M * N$ . With the regular sparse structure of  $T$ , the following  $LU$  decomposition is applied to solve the function.

$$LU = T \quad (4)$$

Where  $L$  is a lower triangular matrix, with non-zero elements only from the main diagonal to the  $M$ th diagonal below the main diagonal. Analogously,  $U$  is an upper triangular matrix, with non-zero elements only from the

main diagonal to the  $M$ th diagonal upper the main diagonal

$$\begin{bmatrix} F(Q(x_1, y_1)) \\ F(Q(x_2, y_1)) \\ \vdots \\ F(Q(x_M, y_N)) \end{bmatrix} = U^{-1}L^{-1}B$$

In this way, the points corresponding to the grid points can be computed. Fig. 8 shows the regular grid warping and the corresponding image results obtained from reshaping some curves of the window part of car body. Since cubic Bézier curve are special cases of B-splines and then of NURBS curve, this method can be used for NURBS curves as well.

For each  $Q(x, y)$  in  $\text{ImgWarp}$ , with  $x_i \leq x \leq x_{i+1}$ ,  $y_j \leq y \leq y_{j+1}$  and the relation

$$F(Q(x, y)) = \frac{y_{j+1} - y}{y_{j+1} - y_j} \left( \frac{x_{i+1} - x}{x_{i+1} - x_i} F(Q(x_i, y_j)) + \frac{x - x_i}{x_{i+1} - x_i} F(Q(x_{i+1}, y_j)) \right) + \frac{y - y_j}{y_{j+1} - y_j} \left( \frac{x_{i+1} - x}{x_{i+1} - x_i} F(Q(x_i, y_{j+1})) + \frac{x - x_i}{x_{i+1} - x_i} F(Q(x_{i+1}, y_{j+1})) \right),$$

each pixel corresponding to  $Q(x, y)$  can be computed as  $F(Q(x, y))$ . The pixel colors of  $\text{ImgWarp}$  can be copied one by one from  $\text{ImgSource}$ .

### 3.5. Optimization

Considering the type of matrices  $L$  and  $U$ , the time complexity for  $LU$  decomposition in equation (4) is

$$O(N * M^3)$$

Reducing the mesh step increases the dimension of  $M$ . Thus, if  $M \leq N$ , the matrices  $T$  and  $B$  will be as defined in section 3.3. Otherwise, the matrix will be changed accordingly. Then, we initialize  $T(M * N, M * N)$

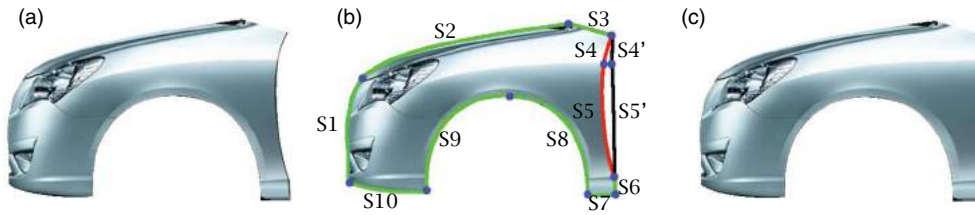


**Figure 9.** Warping results reshaping edges with closed region. (a) is the origin image, (b) is the origin image with the extracted parametric curves (c) illustrates the results modifying curves S4 and S5.

$N$ ) as a unit matrix and  $B(1, M * N)$  as a zero vector. For point  $(x_i, y_j)$ ,  $k = x_i * M + y_j$ , if it is not a constraint point, then

$$T(k, k - N) = -\frac{x_{i+1} - x_i}{x_{i+1} - x_{i-1}} \Big/ 2,$$

$$T(k, k - 1) = -\frac{y_{i+1} - y_i}{y_{i+1} - y_{i-1}} \Big/ 2,$$

$$T(k, k + 1) = -\frac{y_i - y_{i-1}}{y_{i+1} - y_{i-1}} \Big/ 2,$$

$$T(k, k + N) = -\frac{x_i - x_{i-1}}{x_{i+1} - x_{i-1}} \Big/ 2,$$

else

$$B(1, k) = F(Q(x_i, y_j))$$

Thus, in this case the time complexity will be changed to

$$O(M * N^3)$$

In the same way as section 3.4, the correspondence for grid points can be obtained from the matrix solution. Then the correspondence for every pixel can be obtained.

## 4. Results

With the curve driven image warping method described in Section 3, we can obtain many interesting results. For example, in Fig. 9, the curves from S1 to S10 in (b) compose the whole shape of (a). Changing S4 to S4', and S5 to S5', we obtain the warping result shown in (c). In this situation, the warping region is restricted to the region enclosed by the above mentioned edges.

On the other hand, when the restricted region is not a closed region, the warping region is the whole image. Fig. 10 shows the results when dragging one control point to the left in a non limited region. While Fig. 11 shows the warping results obtained reshaping the accent line inside a closed region for the door part.

The above examples demonstrate the capabilities of the method to preserve important characteristics as well: the fixed edges in Fig. 9 and the two inner curves in Fig. 10.

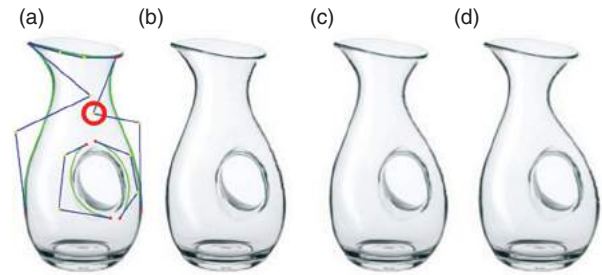


**Figure 10.** Warping results reshaping edges with open region. (a) is the origin image, (b)(c)(d) are results dragging the control point in (a).

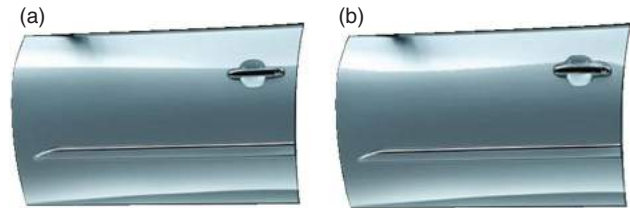


**Figure 11.** Warping result reshaping accent line of the front door.

The method can be applied to edit the image along any curve, according to the user preference. The example shown in Fig. 12 shows the warping effect with reshaping the shadow line.

Since our approach is curve driven image warping, the restricted curve can be kept and the reshaped one has smooth result. Fig. 13 shows the results obtained with our method (Fig. 13(a)), by Photoshop (one of the most used professional image editing software) (Fig. 13(b)) and by the method presented in [14] (Fig. 13(d)) on the car window of Fig. 8. We can see that curves can be easily controlled in the image warping process, while using Photoshop to get the same results would require much more effort. Result in Fig. 13(d) is similar to the result in this paper, but patches (Fig. 13(c)) should be defined firstly to use Ferguson function making the process more complex.

### 4.1. Semantic editing of car images

Considering that given an already specified product, most of the shape modifications are performed to achieve

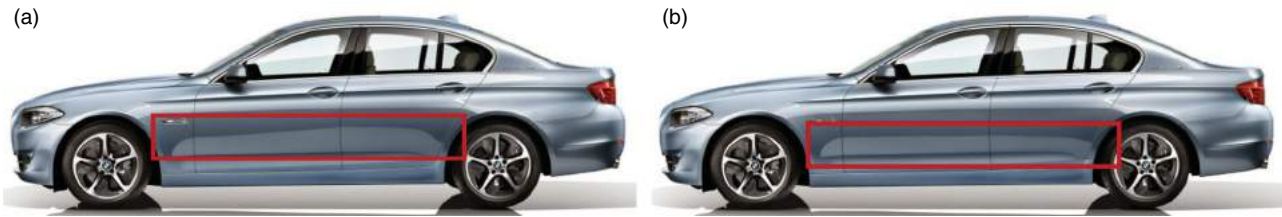


**Figure 12.** Shadow warping; (b) is the reshaped image by changing the shape of the shadow lines in the rectangular area in (a).

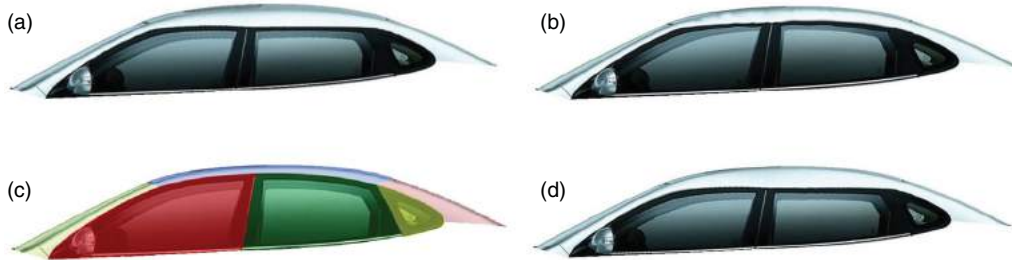


**Figure 13.** (a) Warping result by our method; (b) warping result using *Liquify* filter tool in Photoshop; (d) using method described in [14] based on the patches indicated in (c).

**Table 2.** Aesthetic characters and corresponding presentation modes.

Aesthetic character	Aesthetic key line(s)	Presentation mode	
			Styling
Sportiness	① <i>roof_line</i>		tensed
	② <i>accent_line</i>		sharp or wet
	③ <i>over_wheel_arch</i>		crown
	④ <i>accent_line</i>		tangent to <i>over_wheel_arch</i>
	⑤ <i>rear_overhang_length</i>		shorter
Dynamism	① $\langle ak_l, wheelbase\_line \rangle \in (\beta, \gamma)$		wider
	② <i>windshield_line</i>		more slopped and crown
	③ <i>Roof_line</i>		flattened <i>in the back of the car</i>
Aggressiveness	① <i>hood_line, roof_line, accent_line, crown_line</i>		Accelerated
	② <i>light_contour</i>		sharp
Elegance	① <i>ak_l</i>		tensed, not sharp or wet
	② $ak_{l_i}, ak_{l_j}$		soft conjunction
Friendliness	① <i>over_wheel_arch</i>		sharp, convex, and quite round;
	② <i>ak_l</i>		not tensed
	③ <i>light_contour</i>		convex

or emphasizing a specific character, designers may prefer to manipulate car body model semantically, i.e. specifying the wished car character modification, rather than mathematically acting on the curve control points. Based on the rules defined in [4] and [13] through the discussion with stylists of the most important car industries, the relevant styling properties of aesthetic key lines to aesthetic characters are given in Tab. 2.

Using the automatic extraction method presented in Section 2, the digital model of the car profile can be obtained consisting of the semantically annotated parametric representation of the most important aesthetic key lines. By reshaping the aesthetic key lines (Fig. 14(a), Fig. 15(a)), local semantic-driven model reshaping can be obtained, and the corresponding image warping results (Fig. 14(c), Fig. 15(c)) can then be obtained using

the curve driven image warping method described in Section 3.

In the following, sportiness and dynamism characters are taken as examples to illustrate the semantic-driven model reshaping.

#### 4.1.1. Sportiness character reshaping

According to Tab. 2, if *rear\_overhang\_length* is shorter, the car will look more sporty. Fig. 14(c) shows the image obtained by increasing the sportiness character through shortening the *rear\_overhang\_length* line of the golf car in Fig. 14(b).

#### 4.1.2. Dynamism character reshaping

According to Tab. 2, the aesthetic key lines in the back of the car roof is flatter, the car will appear more dynamic.



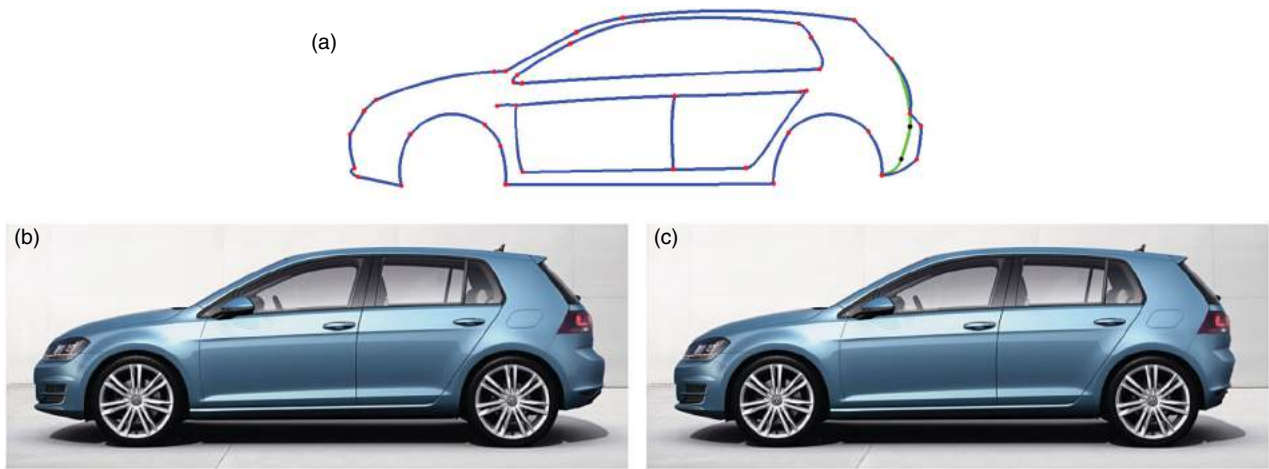


**Figure 14.** Example of reshaping to improve the sportiness character effect. Blue curves in (a) are the automatically detected model from image (b); (c) is the warped image corresponding to the reshaped model driven by green curves shown in (a).

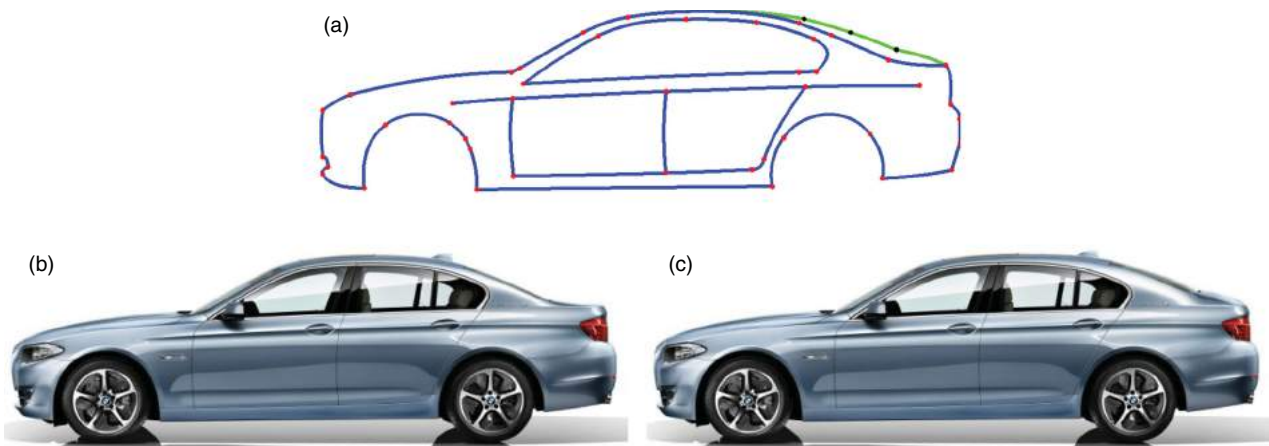


**Figure 15.** Example of reshaping to improve the dynamism character effect. Blue curves in (a) are the automatically detected curve model from image (b); (c) is the warped image corresponding to the reshaped model driven by the roof green curves shown in (a).

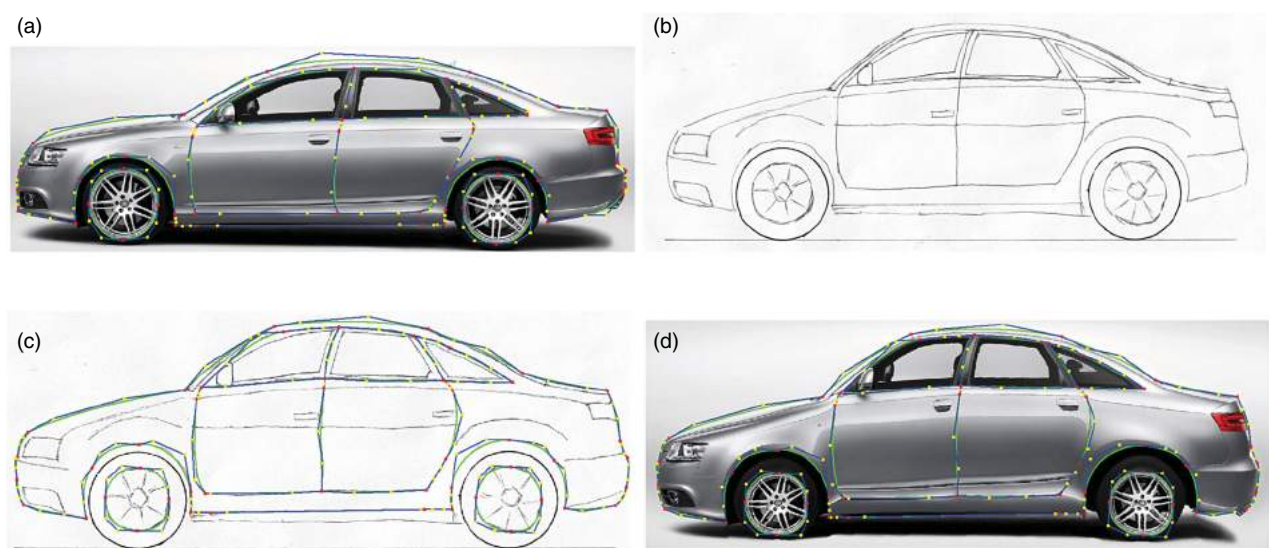


**Figure 16.** Sketch rendering with irregular rectangular mesh warping. Green curves are feature curves represented as Bézier curves with their blue control polygons. (a) Audi A6 rendering image downloaded from website with the extracted Bézier curves; (b) a sketch drawn by a student; (c) the Bézier curves (green) used for the sketch rendering; (d) the sketch rendering result.

Then, Fig. 15, illustrate the result of making the *roof\_line* flatter to achieve the dynamism character reshaping effect.

## 4.2. Car sketch rendering

Using curved boundaries as constraints, the method can be applied to map existing rendering to sketches of similar objects. Fig. 16 shows one of the results obtained applying our warping method for the car sketch rendering. First, the parametric curves corresponding to the characteristic elements of both the textured and the sketch images are computed with the method described in section 2. Then, with user interaction if necessary to adjust the detected curves, and selecting the boundary curves of the warped areas, the sketch rendering effect can be easily obtained. Fast car sketch rendering allows users to better evaluate the impact of sketched car.

## 5. Conclusion

The work presented here provides a contribution towards the direct usage of images for evaluating shape alternatives through an easy modification of the characteristic curves of the product. The work focuses on the identification and modification of characteristic curves in product images. The characteristic curve identification exploits a model template to detect among the curves identifiable in the image the most important from the design point of view. Here, we focused on the car profile characteristic curve detection, but the method can be applied to any product showing certain recurrent characteristic elements that allow the specification of a reference template. The warping method used for the image modification is proven to work well with any type of products as well. Differently from similar approaches, it does not require any constraint on the warping region or on the number of modifiable curves thus allowing the user to manipulate the image according to his own preferences. The method uses irregular meshing for the source and destination images according to the constraint curves firstly; secondly, the inverse mapping is obtained by solving a sparse matrix without using any optimization process as applied by most of the similar works in literature. The application of inverse mapping allows the avoidance of color gaps, thus overcoming similar methods. We finally demonstrate its applicability to the mapping of existing rendering to new product sketches and the possibility of integrating more sematic oriented modelling capabilities.

## Acknowledgements

This project is supported by National Natural Science Foundation of China (Grant No. 11472073, 61370143), the Fundamental Research Funds for the Central Universities (DUT15LK12).

## ORCID

Bo Wang  <http://orcid.org/0000-0003-3497-8931>

Bao-Jun Li  <http://orcid.org/0000-0003-4837-1700>

Franca Giannini  <http://orcid.org/0000-0002-3608-6737>

Marina Monti  <http://orcid.org/0000-0002-1627-3551>

Ping Hu  <http://orcid.org/0000-0002-4467-6841>

Ji-Cai Liang  <http://orcid.org/0000-0001-8881-5949>

## References

- [1] Beier, T.; Neely, S.: Feature-Based Image Metamorphosis. SIGGRAPH '92 Proceedings of the 19th annual conference on Computer graphics and interactive techniques. 26(2), 1992, 35–42. <https://doi.org/10.1145/133994.134003>
- [2] Canny, J.: A computational approach to edge detection, IEEE Transactions on Pattern Analysis and Machine Intelligence, 8(6), 1986, 679–698. <https://doi.org/10.1109/TPAMI.1986.4767851>
- [3] Catalano C. E.; Falcidieno, B.; Giannini, F.; Monti, M.: A Survey of Computer-Aided Modeling Tools for Aesthetic Design, J. Comput. Inf. Sci. Eng, 2(1), 2002, 11–20. <https://doi.org/10.1115/1.1481371>
- [4] Catalano, C.E.; Giannini, F.; Monti, M.; Ucelli, G.: A framework for the automatic annotation of car aesthetics, AI EDAM-Artificial Intelligence for Engineering Design Analysis and Manufacturing, 21(1), 2007, 73–90. <https://doi.org/10.1017/S0890060407070151>
- [5] Dollar, P.; Zitnick, C.L.: Structured forests for fast edge detection. Proceedings of International Conference on Computer Vision (ICCV), 2013, 1841–1848. <https://doi.org/10.1109/iccv.2013.231>
- [6] Eitz, M.; Sorkine, O.; Alexa, M. Sketch Based Image Deformation. Vision, Modeling, and Visualization Conference 2007, Saarbrücken, Germany, November 2007. <http://doi.org/10.1145/2087756.2087775>
- [7] Fontana, M.; Giannini, F.; Meirana, M.: A Free Form Feature Taxonomy, Computer Graphics Forum, 18(13), 1999, 107–118. <https://doi.org/10.1111/1467-8659.00332>
- [8] Hough, P.V.C.: Machine Analysis of Bubble Chamber Pictures, Proc. Int. Conf. High Energy Accelerators and Instrumentation, 1959, 554–558. <https://doi.org/10.1007/BF02733175>
- [9] Karn, Z.; Freedman, D.; Gotsman, C.: Energy-Based Image Deformation. Computer Graphics Forum, 28(5), 2009, 1257–1268. <https://doi.org/10.1111/j.1467-8659.2009.01503.x>
- [10] Lin, S.S.; Yeh, I.C.; Lin, C.H.; Lee, T.Y.: Patch-Based Image Warping for Content-Aware Retargeting, IEEE Transactions on Multimedia, 15(2), 2012, 359–368. <https://doi.org/10.1109/TMM.2012.2228475>
- [11] Ma, J.Y.; Zhao, Ji.; Yuille A.L.: Non-Rigid Point Set Registration by Preserving Global and Local Structures, IEEE Transactions on Image Processing, 25(1), 2016, 53–64. <https://doi.org/10.1109/tip.2015.2467217>
- [12] Orbay, G.; Yümer, M. E.; Kara, L. B.: Sketch-based aesthetic product form exploration from existing images using piecewise clothoid curves, Journal of Visual Languages & Computing, 23(6), 2012, 327–339. <http://doi.org/10.1016/j.jvlc.2012.07.001>
- [13] Wang, B.; Li, B.J.; Hu, P.; Song, M.L.: Semantic-Oriented Shape Exploration for Car Styling, International

- Conference on Digital Home, 2014, 368–373. <https://doi.org/10.1109/ICDH.2014.75>
- [14] Wang, B.; Li, B.J.; Hu, P.; Song, M.L.; Liang, J.C.; Yang, L.: An Effective Image Reuse Approach for Product Styling, *Journal of Information and Computational Science*, 12(1), 2015, 235–246. <https://doi.org/10.12733/jics20105193>
- [15] Wang, Y.S.; Tai, C.L.; Sorkine, O.; Lee, T.Y.: Optimized Scale-and-Stretch for Image Resizing, *ACM Transactions on Graphics (TOG) - Proceedings of ACM SIGGRAPH Asia* 2008, 27(5): Article 118. <https://doi.org/10.1145/1457515.1409071>
- [16] Wolberg, G.: Image morphing: a survey, *The Visual Computer*, 14(8), 1998, 360–372. <https://doi.org/10.1007/s003710050148>
- [17] Zhou, S.Z.; Fu, H.B.; Liu L.L.; Cohen-Or, D., Han, X.G.: Parametric Reshaping of Human Bodies in Images, *ACM Transactions on Graphics (TOG) - Proceedings of ACM SIGGRAPH* 2010, 29(4): Article 126. <https://doi.org/10.1145/1833349.1778863>